Preparation and Characterization of Nanostructured and High Transparent Hydrogel Films with pH Sensitivity and Application

Yumei Yue,[1,2] Pixin Wang,[2] Qiang Chen,[2] Xiao Guang Liu[2]

[1]*Engineering Research Center of Pesticide, Heilongjiang Province, Heilongjiang University, Harbin 150080, People's Republic of China*
[2]*Changchun Institute of Applied Chemistry, Chinese Academy of Sciences, Changchun 130022, People's Republic of China*

Received 5 November 2007; accepted 23 November 2008
DOI 10.1002/app.29773
Published online 13 February 2009 in Wiley InterScience (www.interscience.wiley.com).

ABSTRACT: Novel nanostructured, high transparent, and pH sensitive poly(2-hydroxyethyl methacrylate-*co*-methacryliac acid)/poly(vinyl alcohol) (P(HEMA-*co*-MA)/PVA) interpenetrating polymer network (IPN) hydrogel films were prepared by precipitation copolymerization of aqueous phase and sequential IPN technology. The first P(HEMA-*co*-MA) network was synthesized in aqueous solution of PVA, then followed by aldol condensation reaction, it formed multiple IPN nanostructured hydrogel film. The film samples were characterized by IR, SEM, DSC, and UV-vis spectrum. The transmittance arrived at 93%. Swelling and deswelling behaviors showed the multiple IPN nanostuctured film had rapid response. The mechanical properties of all the IPN films improved than that of PVA film. Using crystal violet as a model drug, the release behaviors of the films were studied. The results showed that compared with PVA, which had low drug loading and exhibited high and burst release, the three IPN films had high drug loading and exhibited sustained release. Besides, the release followed different release mechanism at pH = 4.0 and pH = 7.4, respectively. © 2009 Wiley Periodicals, Inc. J Appl Polym Sci 112: 2261–2269, 2009

Key words: interpenetrating networks (IPN); pH-sensitive polymers; transparent; films; drug delivery; nanostuctured

INTRODUCTION

Polymer hydrogels have a great interest for pharmaceutical and medical applications.[1–3] The water uptake of hydrogels is sensitive to external environment, including the temperature, the pH, the ionic strength, and the electric field. Therefore, they are extensively applied in biomedical field. Poly (2-hydroxyethyl methacrylate) (PHEMA) was the first hydrogel for biomedical applications in 1960s.[1] To date, these gels have been largely used in biomedical applications[4,5] and as separation or adsorption matrices for various metal ions.[6,7] However, many of their potential applications are hindered by their limited water uptake,[8] low mechanical strength, and slow response rate.[9,10] To improve the water swelling property of PHEMA hydrogels, various monomers which are more hydrophilic than HEMA are introduced such as vinylpyrolidone[11] and ethylene glycol methacrylate.[12] Many efforts are attempted to enhance the swelling and deswelling rates of the hydrogels, such as the introduction of combtype-grated chain[13] or porous structure[14,15] into the network.

Formation of interpenetrating polymer networks (IPNs) could be a possible solution to resolve aforementioned problem. An IPNs is defined as a combination of two polymers in network form, at least one of which is synthesized and/or cross-linked in the immediate presence of another polymer. The interlocked structures of the cross-linked components are believed to ensure stability of the bulk and surface morphology. By using IPN method, thermodynamic incompatibility can be overcome because fo permanent interlocking of network segments and IPNs with limited phase separation can be obtained. Some IPNs of based-PHEMA was prepared to enhance the water uptake[16,17] and response rate,[18] such as polyvinyl alcohol[16] and gelatin.[17] Although HEMA is soluble in water, but PHEMA is not soluble in water and has limited compatibility with these polymers and solvent,[19,20] the preparation of their hydrogels are limited in bulk or high monomer content, or using organic solvent such as DMF and DMSO. Especially, visually clear hydrogel has only been obtained at high HEMA content[9] (>60%) or in organic solvent (isopropyl ether).[21] When the water swelling ratio is in the range of 0.92–0.93, the hydrogel they prepared is transparent. Only one

Correspondence to: P. Wang (pxwang@ciac.jl.cn).

transparent polymer membrane of PHEMA was prepared in microemulsion.[22] It is temperature-sensitive ternary copolymer of PMMA-*co*-PHEMA-*co*-PNIPAM for wound dressing and cell grating. Water is used as reactant solvent, which accorded with the characteristic of green chemistry. Especially, for hydrogel for biomedical applications, it has obvious advantages such as avirulence and easy purification.

The pH sensitive hydrogels have attracted great attentions in recent years both in fundamental and technological interests. These materials are useful for drug delivery systems, separations in biotechnology, and so on. In these applications, a fast response rate and good mechanical property of the hydrogel to the external stimuli are needed.

Poly(vinyl alcohol) (PVA) is a water soluble poly hydroxyl polymer, widely used in practical applications in biomedicine and biochemistry because of easy preparation, excellent chemical resistance, biocompatibility, and complete biodegradability. However, because PVA, PMA, and PHEMA are not compatibility of each other in aqueous solution, in this study, we used precipitation copolymerization of aqueous phase and interpenetrating polymer networks idea to prepare novel nanostructured, high transparent, and pH-sensitive hydrogel films. P(HEMA-*co*-MA) as the first network was synthesized and precipitated in the presence of PVA aqueous solution, then using aldol condensation reaction, which made the microphere moored in the matrix of the film and formed nonastructured hydrogel films with multiple interpenetrating network. When compared with other visually clear PHEMA hydrogel, the novel high transparent hydrogels film contained PHEMA with high water content were obtained. This method used water as reaction medium, avoided using organic solvent and overcame the compatibility problem of PHEMA. Using crystal violet as model drug, the release behaviors of the films were investigated.

EXPERIMENTAL

Materials

2-Hydroxyethyl methacrylate (HEMA, E. Merch Darmstadt, GE) and methacrylic acid (MA), analyst reagent (Beijing chemical plant'China), were distilled under reduced pressure before use. Poly (vinyl alcohol) (PVA, 87–89% hydrolyzed, molecular weight 88,000–97,000 g/mol), Ethylene glycol dimethacrylate (EGDMA) was purchased from Alfa Aesar, A Johnson Matthey Co. N′N′N′N′-Tetramethylethylendiamine (TMEDA, 99%) was from Aldrich chemicals (USA). Crystal violet (CV) was supplied by Fluka (USA). Glutaraldehyde (GA, 25%aq. Soln) was provided with Avocado Research Chemicals Ltd (UK). Ammonium persulfate (APS) and hydrochloric acid were obtained from Beijing chemical plant (China). Except for MA and HEMA, all other regents of analytical grade were used as received.

TABLE I
Feed Composition used for the Polymerization

	Compositions by wt %[a]			
Symbol	HEMA	MA	PVA	H_2O
IPN1	1.625	0.875	2.5	95
IPN2	1.25	1.25	2.5	95
IPN3	0.875	1.625	2.5	95

[a] The crosslinker (EGDMA): 1.0% molar to total monomer.

Preparation of P(MA-*co*-Hema)/PVA IPN films

The feed composition menu for the preparation of the IPN was showed in Table I. About 100 g of each solution consisting of water, MA, HEMA, EGDMA, PVA, and TEDMA were used to prepare the nanostructured IPN films. Each mixture was degassed 30 min by nitrogen purging prior to the addition of the initiator, APS (0.35 mol% to total monomer). Then the polymerization was standing 24 h at 50°C under stirring and nitrogen atmosphere. After polymerization, 1.0 wt % GA in weight of PVA and 1*N* HCl with GA same weight were added. At room temperature, after 1 h the solution were transferred into a known area petri dishes and dried for 8 h at 50°C in an oven. The film obtained was immersed in water for 2 days, to eliminate any possible residual matter, and then dried under vacuum at 30°C for 3 days.

Morphology studies

Scanning electron micrographs of the films were taken with a scanning electron micrograph (XL30 ESEM FEG). The cross sections of the films were observed and photographed after cracked in liquid N_2 and sputter-coated with a thin layer of gold.

FTIR studies

Attenuated total reflectance-fourier transform infrared spectroscopy (ATR-IR) of the film samples was measured with Bruker Vertex 70 FTIR spectrophotometer, the spectra were signal averaged over 128 scans at a resolution of 2/cm, detector is DTGS.

Thermal characterization

DSC (differential scanning calorimetry) was measured on PE 7 Series Thermal Analysis System (USA). About 10 mg films were scanned from 20 to 200°C

at a heating rate of 10°C/min under N_2 flow. The first scan was used to remove the hot history, the T_g and T_m were obtained from the second scan. The T_g value was taken from the midpoint of the special heat increment, and the T_m value was taken from the peak value of the melting curve, respectively.

Transparency (T%) measurements

Optical transparency of the films was measured by the transmittance of the water-swollen sample. The transmittance of about 0.3 mm thick hydrolgel film was recorded with by UV/VIS/NIR spectrometer (Perkin–Elmer Lambda 900, USA)from 800–200 nm.

Swelling and deswelling studies[23]

The equilibrium swelling of the films was measured after the preweight dried films were swollen to the equilibrium state in buffer solution of different individual pH at room temperature. The swollen film was weighed after being slightly removed from the surface water by filter paper. The swelling ratio was calculated by the following equation: swelling ratio = $(W_s - W_d)/W_d$, where W_d is the weight of dried film, and W_s is the weight of swollen film.

The deswelling kinetics of hydrogel film was studied by pH sensitivity when the swollen film at pH = 7.0 was transferred into pH = 2.0 phosphate buffer by measuring film weight at different time. Swelling ratio was calculated by the equation: swelling ratio = $(W_t - W_d)/W_d$, where W_t was the weight of hydrogel film at a given time during deswelling at pH = 2.0, W_d was the weight of dried film. And when t = 0, W_t was the weight of swollen hydrogel at pH = 7.0, it was beginning of deswelling.

Mechanical properties

The tensile measurement was conducted on INSTRON 1121(USA)material test machine with a tensile rate of 20 mm/min at room temperature. After the films were fully swelled in water, the sample strips were 40 mm length and 10 mm width with 20 mm distance between the two clamps. Three or four measurements were carried out for every sample and the mean value was obtained.

Drug release studies

Crystal violet was used as a model drug. About 30 mg dried films were equilibrated in drug solution of 30 mg/10 mL distilled water at room temperature for 2 days to load drug into the films. Then the loaded-drug gels were removed from the drug solution and dried under vacuum at 30°C for 3 days. The drug loading amount was calculated by the following equation: the drug loading amount = $(W_l - W_d)/W_d \times 100$, Where W_d is the weight of dried sample, and W_l is the weight of drug loaded samples.

The drug release experiment was carried out by transferring the dried drug-loaded films in 10 mL buffer solution of different pH at 37°C. The IPN films loaded with CV were placed in the desired release medium and repeatedly removed from the solution, then transferred into 10 mL fresh release medium at each fixed time interval. The released drug was analyzed by ultraviolet spectrophotometer (Perkin–Elmer Lambda 900, USA)at 598nm. The release amount was calculated by previously established calibration curve.

RESULTS AND DISCUSSION

Preparation of P(Hema-*co*-MA)/PVA IPN films

In this study, the general procedure for the preparation of the novel pH sensitive, nanostructured and high transparent IPN hydrogel film was showed in Scheme 1. Because PVA, PMA, and PHEMA are not compatibility of each other in aqueous solution, in the first step, HEMA and MA were copolymerized using EGDMA as a crosslinker in the present of PVA aqueous solution. After polymerization started, the copolymer micropheres of P(HEMA-*co*-MA) precipitated from the system. PVA, as one of the network compositions, was mainly act as stabilizing agent in the first stage to stabilize the precipitated particles of P(HEMA-*co*-MA) and the reactant solution was homogeneous and steady latex in the action of PVA.

After the formation of the first copolymer networks, in the second stage, the crosslinker GA was added. GA could react both with the OH of PVA and the OH of PHEMA in P(HEMA-*co*-MA), therefore three new networks formed. These were: one network formed by PVA with GA, one network formed by PHEMA with GA, one network formed by PVA and PHEMA with GA. Especially, the network formed by PHEMA and PVA with GA made the microspheres of P(HEMA-*co*-MA) studded in the matrix of the IPN film and formed the bulk nanostructure. If in the second stage, GA was not added, the micropheres of P(HEMA-*co*-MA) were again floated in water when the dried films were immersed in water and finally the film samples would not be obtained to further use. This confirmed the role of GA.

Microscopic studies

The photographs of cross sections (Fig. 1) also confirmed the nanophase structure, which more exactly

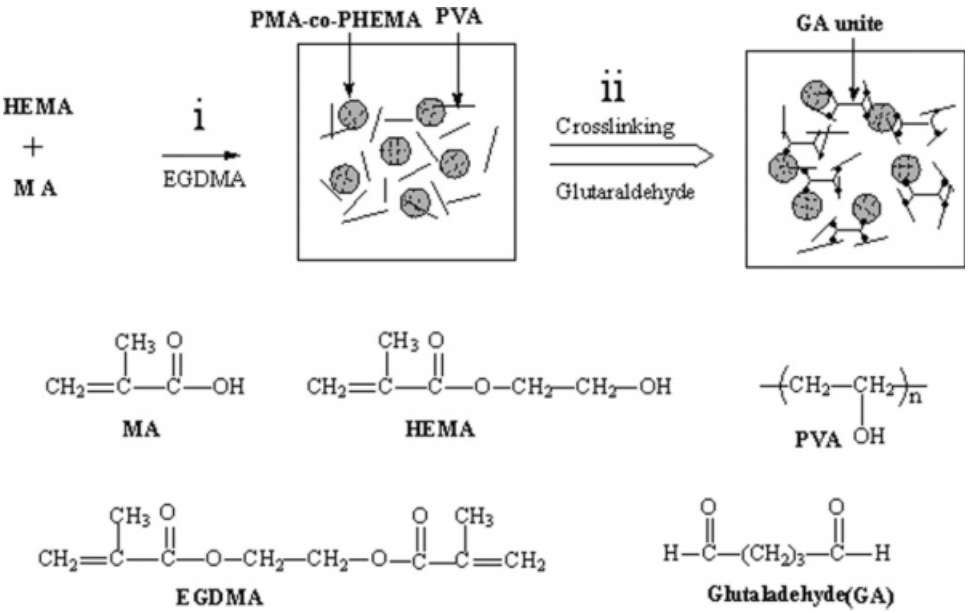

Scheme 1 Schematic diagram illustrating the processes for the preparation of P(MA-*co*-HEMA)/PVA IPN via precipitation polymerization and aldol condensation reaction. (i) HEMA and MA were copolymerized and precipitated using EGDMA as a crosslinker in the present of PVA aqueous solution. (ii) The nanostructured, pH sensitive, and multiple IPN transparent film was formed by aldol condensation reaction between Glutaraldehyde (GA) and hydroxyl group(OH).

exhibited that the GA crosslinker made the copolymer microspheres of P(HEMA-*co*-MA) formed in the first precipitation polymerization stage, moored in the IPN matrix. At the same time, it could also be observed that the size of the microspheres increased with the increase of PHEMA content. It was may be that of higher content PHEMA in the P(HEMA-*co*-MA), more hydrophilic of the copolymer spheres

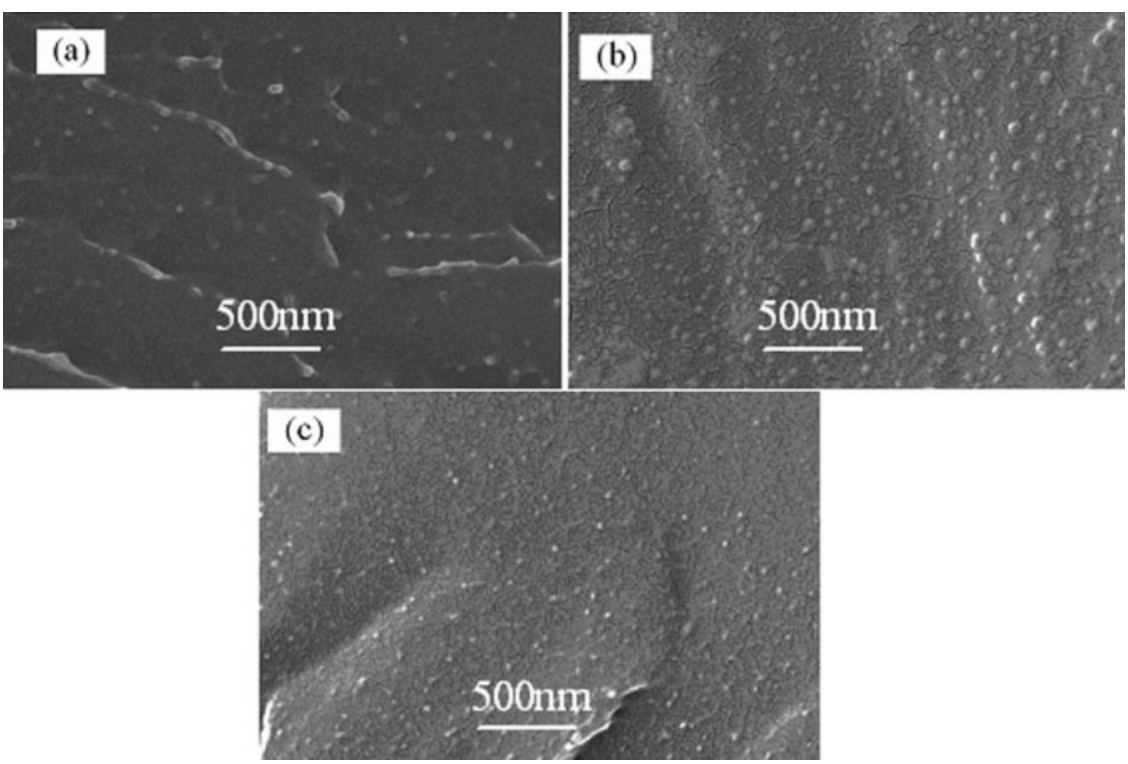

Figure 1 SEM photographs of the cross section of different compositions of the IPN films, (a) for IPN1, (b) for IPN2 and (c) for IPN3, respectively.

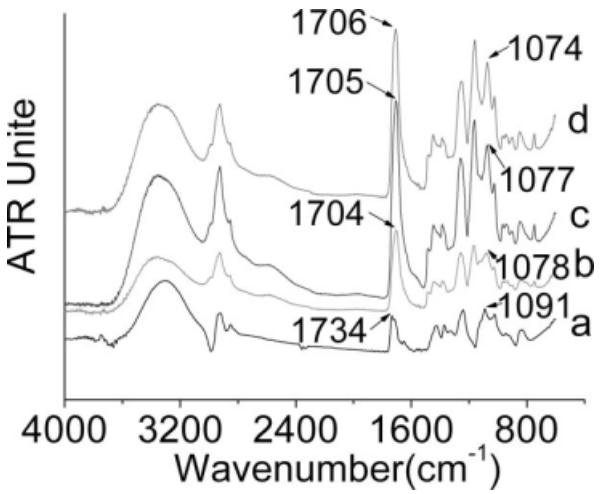

Figure 2 ATR-FTIR spectra of PVA, P(MA-*co*-HEMA)/PVA IPN films. (a) PVA, (b) IPN3, (c) IPN2, (d) IPN1.

and induced particle diameter to grow up larger. The particle size ranged from about 10 nm to 40 nm for IPN3 to IPN1.

The ATR- FTIR spectra

The ATR-IR spectra of PVA and IPN films were presented in Figure 2. Comparison with the IR spectrum of PVA, the IR spectra of P(HEMA-*co*-MA)/PVA IPN films had evident change. The C=O stretching vibration, in PVA at 1734/cm (residual acetate group of PVA), was 1706/cm in IPN1. Besides, the broad peak of 3600–2500 was COOH characteristic peak of PMA of P(HEMA-*co*-MA)/PVA IPNs, which overlapped with OH stretching.

Because of the hydrogen bond interactions, the dissymmetry stretching vibration of C=O at 1706/cm in IPN1 shifted to low wave number in the IPNs with decreasing HEMA content, and C—O stretching vibration in the region of 1000–1300/cm shifted to higher wave number with a decrease of HEMA content in feed composition. For example, the wave number of the C—O peak from 1074/cm for IPN1, shifted to 1077/cm,1078/cm at IPN2, IPN3 respectively. These showed the results of new intermolecular hydrogen bond interactions of IPNs and new IPN formed.

Thermal properties

The miscibility of polymer blends with one semicrystalline component can be determined by melt point depression. Thermodynamic considerations predicted that the chemical potential of polymer will decrease by addition of miscible dilute. If one polymer was crystalizable, its decrease in chemical potential will result in a decreased equilibrium melting point.

From the DSC measurement (Fig. 3), for IPN1 a single glass transition temperature (T_g) and a T_m were observed. Compared with pure PVA in which DSC curve exhibited a T_m at 181.7°C, the T_m decreased to 167.5°C, and at the same time the peak area also decreased. This indicated that the IPN network components are miscible in their melt states.[24–26] For IPN2 and IPN3, only a single T_g was observed, but the T_m peak disappeared because of specific endothermic and exothermic interactions. In addition, T_g s of the IPNs decreased with increasing HEMA content. Generally, a single T_g between the two networks of this IPN can be used to estimate the miscibility between two networks of an IPN.[27–30] The single T_g of the IPN films versus composition-dependent relationship further indicated the miscibility.

From DSC analysis, it can be seen that this preparation method make mutually incompatible composition of PVA, PHEMA, and PMA turn to completely thermodynamically miscible. The good compatibility attributed to the formation of covalent bonding formed by PHEMA and PVA with GA. Namely, the macroscopically even nanophase structure make IPN films excellent miscibility.

Transparency (T %) measurements

The IPN films were transparent and pH-sensitive in their swelling ratio. Figure 4 illustrated the transparency of the water-swollen hydrogel films by recording the transmittance scanning from 800 nm to 200 nm using air as a blank (it was defined as 100%). For IPN1, the swollen film was almost transparent, but slightly opalescent. When below 450 nm, the transmittance was less than 70%. For IPN2 and IPN3, the nanostructured films were completely

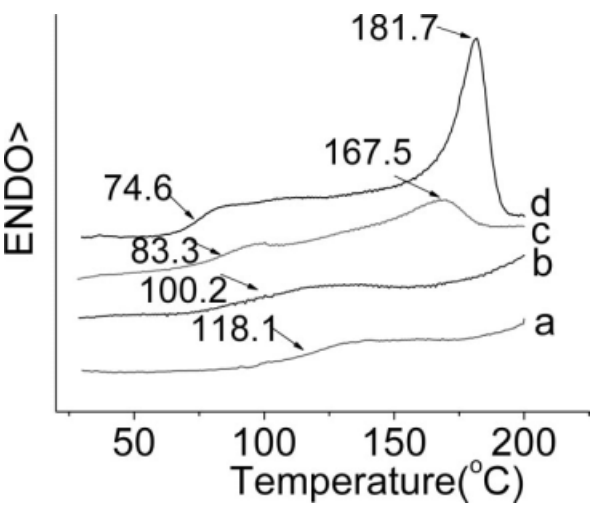

Figure 3 DSC curves of P(MA-*co*-HEMA)/PVA IPN films. (a) IPN3, (b) IPN2, (c) IPN1, (d) pure PVA.

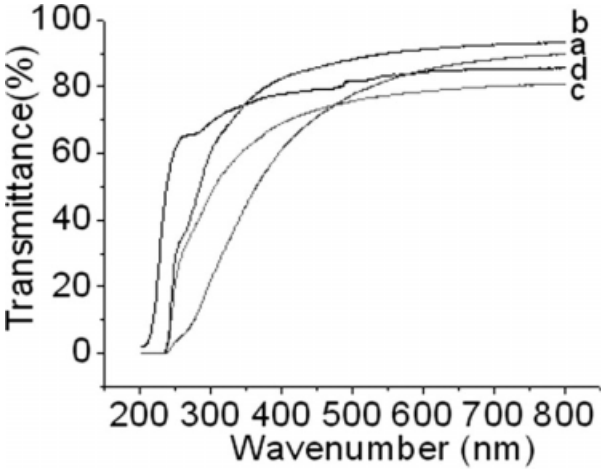

Figure 4 The UV-vis spectra of the swollen P(MA-*co*-HEMA)/PVA IPN films and PVA. (a) IPN3, (b) IPN2, (c) IPN1, (d) PVA.

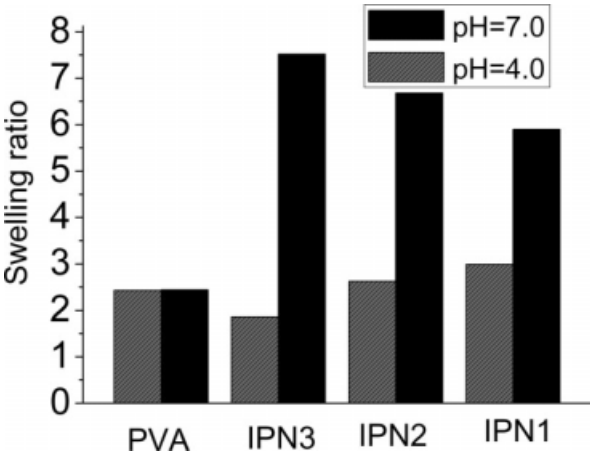

Figure 6 The equilibrium swelling ratio of films at different pH.

transparent in fully swelling states (Fig. 5). Especially the IPN2 (curve b), the highest transmittance arrived to 93% at 800–760 nm, however, its transmittance was still high to 80% even though at 380 nm. Comparison with pure PVA film, in general, the nanophase structure of IPN films had no effect on the transparency and the IPN films were still in high transparency.

Swelling and deswelling studies

The swelling behavior was important parameter to the hydrogel. As can be seen from Figure 6, it was difference with PVA, which equilibrium swelling ratio was almost not changed with pH changing, for three IPN films the equilibrium swelling ratio at pH = 7.0 was higher than pH = 4.0. Moreover, the equilibrium swelling ratio increased at pH = 4.0, but decreased at pH = 7.0 with increasing PHEMA content (decreasing PMA content). The trend was on the contrary. Because of the presence of carboxylic acid, the swelling behavior of the hydrogel contained PMA was highly dependent on the pH of the surrounding medium. The pK_a of PMA was 5.65, so in pH 4.0 acetate buffer solution, the carboxyl groups of PMA was at a hydrated state, the swelling ratio mainly rested with the hydrophilicity, thus increased with increasing PHEMA content because of the hydrophilicity of PHEMA stronger than that of PMA. In pH 7.0 phosphate buffer solution, because of the ionic repulsion of carboxylic ions (COO^-), here, which was dominating factor and induced the significant increase of the water uptake, therefore the highest swelling ratio of IPN film was achieved at pH 7.0 and increased with increasing PMA content.

The deswelling kinetics of hydrogel films was measured by pH sensitivity when the swollen

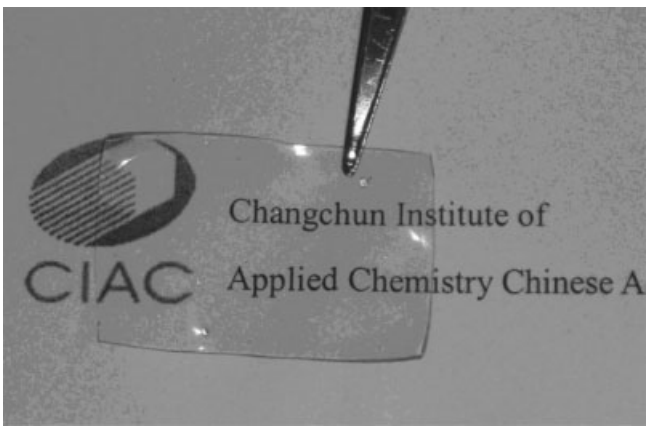

Figure 5 A photograph of a typical transparent film (IPN2).

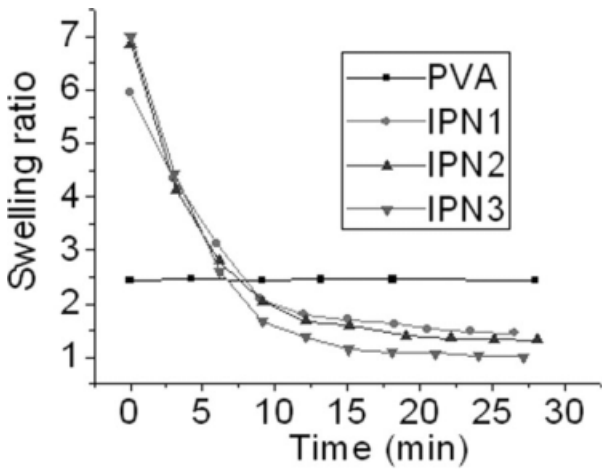

Figure 7 Deswelling kinetics of IPN films and PVA (pH = 2.0). Swelling ratio changed as a function of time.

TABLE II
Mechanical Properties and Drug Loading Amount of P(MA-co-HEMA)/PVA Films and PVA

Symbol	IPN1	IPN2	IPN3	PVA
Tensile strength (MPa)	0.63 ± 0.05	0.66 ± 0.16	1.13 ± 0.08	0.44 ± 0.09
Elongation at break (%)	90 ± 12	171 ± 30	202 ± 20	78 ± 32
Young's modulus (kPa)	725 ± 56	388 ± 12	565 ± 31	332 ± 30
Drug loading (%)	19.08	21.12	24.02	6.34

samples were transferred from pH = 7.0 into pH = 2.0 phosphate buffer. Because the ionic repulsion of carboxylic ions (COO^-) of PMA at pH = 7.0 was above its pK_a 5.65, it induced the significant increase of water uptake. Below its pK_a the protonation of carboxyl groups of PMA decreased the water sorption, so the water can release from the network. So the deswelling can occurred. Figure 7 exhibited the deswelling behavior for all the samples. Compared with the PVA, which swelling degree was almost not affected by pH, so it did not occur to deswelling, but the IPN films exhibited rapid deswelling rate due to its pH sensitivity which the second P(HEMA-*co*-MA) network bestowed on. This displayed the advantage of interpenetrating networks. The PVA network gave full play to good film-forming ability and P(HEMA-*co*-MA) network provided the IPN film with pH sensitivity. They almost lost about 95% water they can lose at 15 min and almost at the same time reached the deswelling equilibrium in 30 min.

When the IPN hydrogel films were transferred from pH = 7.0 to pH = 2, the carboxylic ions of PMA segments of P(HEMA-*co*-MA) located in the outer surface first occurred deionization and started to deswell.[31] The hydrogel shrank immediately. Here, ionic state (COO^-) of the outer surface PMA transferred as carboxyl groups (COOH). This induced free volume decreases and the water molecules released from the networks. Because of the fast shrinking of P(HEMA-*co*-MA) particles in the surface regain, many cavities appeared, which formed interconnected channels to available water fast diffuse out. So a large amount of free water rapidly released from the networks. And thus because of the nanostructure the IPN films exhibited rapid deswelling rate.

From Figure 7, we also see that the high PMA content with high swelling ratio at pH = 7.0 but low swelling ratio at pH = 2.0. The result of low PMA content was contrary to that of high PMA content. But all the IPN films almost simultaneously reached the equilibrium state. It showed that the film of high PMA content had faster deswelling rate and more sensitive to pH.

Mechanical properties of P(MA-*co*-Hema)/PVA IPN films

Good mechanical properties would be expected for application of materials. In this study, tensile strength, elongation at break and Young's modulus were measured to determine the mechanical properties of these IPN films. The films had similar mechanical behavior of rubber elasticity in their swelling state. As shown in Table II, the mechanical properties of all the IPN films with different compositions improved than that of PVA film. Tensile strength and elongation at break slightly increased with a decrease of HEMA content. The IPN3 had the highest tensile strength and elongation at break, 1.13 MPa and 202%, respectively. But Young's modulus was lowest at IPN2 in IPN films. Comparison with PVA film, the IPN film had better flexibility and higher strength, indicating the IPN film exerted the coordinated effect of the interpenetrating polymer network.

Drug release study

Cationic compound crystal violet (CV) was used as a model drug to investigate the drug release from the film at different pH at 37°C.

Figure 8 showed the FTIR spectrum of drug loaded film, the FTIR spectra of blank IPN film and crystal violet (CV) were included for comparison. The characteristic peaks of CV at 1581/cm and 1358/cm were the stretching vibration of phenyl

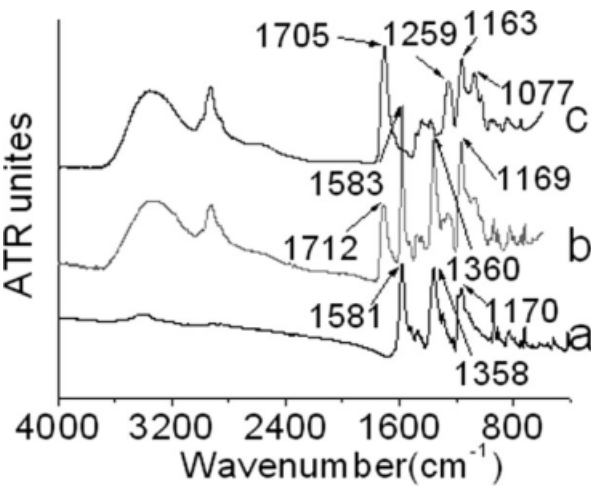

Figure 8 FTIR spectra of crystal violet (a), films loaded with CV (b), and blank P(MA-*co*-PHEMA)/PVA IPN films (IPN2) (c).

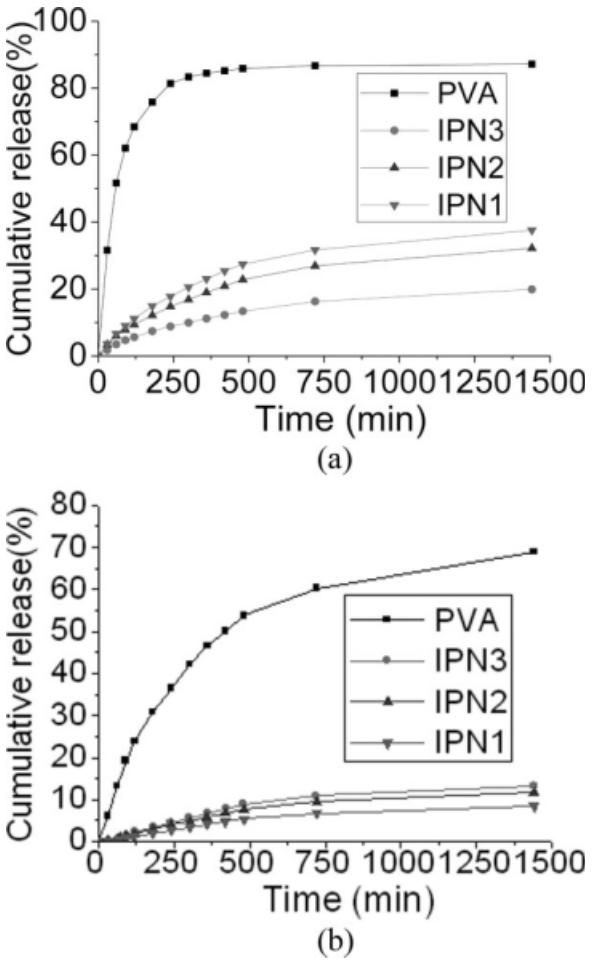

Figure 9 Crystal violet release profiles of P(MA-*co*-HEMA)/PVA IPN films and PVA film at 37°C. (A) In pH = 4 acetate buffer solution; (B) In pH = 7.4 phosphate buffer solution.

framework and the stretching vibration of CH_3, respectively. And the stretching vibration at 1701/cm was due to C—N bond. Through curve b (Fig. 8) we can see that the characteristic absorption peaks of curve c at 1705/cm and 1259/cm had shifted to higher wavenumber at 1712/cm and 1263/cm, respectively. The results indicated that the model drug CV had strong intermolecular interactions with the matrix of the IPN film. At the same time, from Table II, we can see that the drug loading amount of IPN film increased with increasing PMA content, besides, higher than that of PVA film. The reason should mainly be the interaction of electrostatic attraction between the CV and PMA.

At pH = 4.0 and pH = 7.4, the release profiles of crystal violet were showed in Figure 9. Compared with PVA, which had high and burst release, for the three IPN films the release exhibited sustained character because to the interaction between the CV with PMA. This also displayed the advantage of interpenetrating networks. At pH = 4.0 [Fig. 9(A)], the CV release rate decreased with the increase of PMA content. Namely, the higher drug loaded, the lower the drug release rate was. At pH = 7.4 [Fig. 9(B)], the relationship of the CV release rate with network compositions was on the contrary with pH = 4.0, the release amount increased with the increase of PMA content. Therefore changing pH can adjust its release.

The equation of $M_t/M_\infty = kt^n$ was used to study the release kinetics,[32] where M_t/M_∞ represented the drug release fraction at time t, k was a constant incorporating the structural and geometric characteristics of the matrix tablets, and n was the release exponent, indicative of the drug release mechanism. When $n = 0.5$, it was Fickian release; $n = 1$, it was zero order release; $1 > n > 0.5$, it was non-Fickian release or anomalous transport of drug (diffusion and polymer relaxation simultaneously make effect). To clarify the release exponent, the ln value of the percentage drug release was plotted against ln t according to equation of $\ln(M_t/M_\infty) = \ln k + n \ln t$. A straight line could be gotten and n values were summarized in Table III. From Table III, we can see that n values were between 0.5 and 1 at pH = 4.0, it meant that the swelled hydrogel matrix released drug following the diffusion and polymer relaxation mechanism for IPN films. Because of the strong bind of cationic CV with PMA of hydrogel matrix, in acid medium the diffusion of H^+ into the loaded film matrix enhanced the positive charge of the IPN network, thus caused electrostatic repulsion and subsequently relaxation of polymer chains which accelerated CV dissociation from the polymer chains and diffusion from hydrogel matrix into outer medium. So a greater swelling ratio, a faster release rate was.

At pH = 7.4, the n values were >1, the drug release was accelerated course for IPN films. At pH = 7.4, hydrogel matrix first occurred to ionization and the carboxyl groups (COOH) transferred to carboxyl ions (COO^-). Because CV was cationic and here hydrogel film was anionic property, the electrostatic attraction between the drug and hydrogel film was dominant factor of influencing release. In basic medium, at the beginning electrostatic attraction of CV with of COO^- of PMA didn't make CV dissociated from the matrix of films, but the film first swelled due to ion repulsion of carboxyl of PMA. Simultaneously, electrostatic attraction of CV with of

TABLE III
***n*-Values Obtained for Drug Fractional Release of P(MA-co-HEMA)/PVA IPN Films**

	pH = 4.0		pH = 7.4	
Symbol	n	R^2	n	R^2
PVA	Nonlinear	–	Nonlinear	–
IPN1	0.6933	0.9898	1.1675	0.9817
IPN2	0.654	0.9952	1.1095	0.9875
IPN3	0.6853	0.9872	1.1426	0.979

COO^- of PMA limited the relaxation of network chains. So with the swelling increasing and the diffusion of OH^+ ions into the film matrix, which could partially nullify the positively charged CV, the cationic drug released from the hydrogel matrix into the medium with an accelerated rate. Swelling degree and drug-loaded amount increased with PMA content increasing, and therefore the release amount and rate increased at pH 7.4.

CONCLUSIONS

A novel strategy was proposed to fabricate novel stimulate (pH)-sensitive, nanostructured high transparent hydrogel films with rapid response rate by using precipitation polymerization of aqueous phase and interpenetrating networks idea. SEM analysis confirmed the copolymer nanoparticles studded in the IPN matrix formed the bulk nanostructure. The spectra of ATR-FTIR showed new intermolecular interaction hydrogen bonds of the IPNs. DSC analysis showed this method made mutually incompatible of PVA, PHEMA and PMA turn to completely thermodynamic miscible. The highest transmittance arrived to 93%. The three IPN films exhibited rapid deswelling behavior due to the nanostructure and improved mechanical properties. The application of the film materials in controlled drug delivery field was investigated using crystal violet as a model drug. We found that comparison with PVA which exhibited high and burst release, for three IPN films the drug release was sustained character. Besides, the release followed different release mechanism at pH = 4.0 and pH = 7.4, respectively. These results fully exhibited the advantages of interpenetrating polymer networks and coordinated effect of various compositions.

References

1. Wichterle, O.; Lim, D. Nature 1960, 185, 117.
2. Sheena, A.; Sean, B.; Kazuhiko, I.; Anthony, G. E. Biomaterials 2005, 26, 4767.
3. Liu, Y.Y.; Lü, J.; Shao, Y. H. Macromol Biosci 2006, 6, 452.
4. Kanadag, E.; Saraydin, D.; Centinkaya, S.; Güven, O. Biomaterials 1996, 17, 67.
5. Yu, T.; Ober, C. K. Biomacromolecules 2003, 4, 1126.
6. Akgöl, S.; Kuşvuran, E.; Kara, A.; Şenel, S.; Denizli1, A. J Appl Polym Sci 2006, 100, 5056.
7. Denizli, A.; Say, R.; Testereci, H. N.; Arica, M. Y. Sep Sci Technol 1999, 34, 2369.
8. Nakamura, K.; Nakagawa, T. J Polym Sci Polym Phys Ed 1975, 13, 2299.
9. Atta, A. M.; Arndt, K. F. Polym Int 2004, 53, 1870.
10. Chou, L. Y.; Blanch, H. W.; Prausnitz, J. M.; Siegel, R. A. J Appl Polym Sci 1992, 45, 1411.
11. Kabra, B. G.; Gehrke, S. H.; Hwang, X. T.; Ritschel, W. A. J Appl Polym Sci 1991, 42, 2409.
12. Lee, W.; Lin, W. J. J Polym Res 2002, 9, 23.
13. Ju, H. K.; Kim, S. Y.; Lee, Y. M. Polymer 2001, 42, 6851.
14. Chen, J.; Park, H.; Park, K. J Biomed Mater Res 1999, 44, 53.
15. Serrano, A. A.; Campillo Fernández, A. J.; Gómez Ribelles, J. L.; Monleón, P. M.; Gallego, F. G.; Pissis, P. Polymer 2004, 45, 8949.
16. Ramaraj, B.; Radhakishnan, G. Polymer 1994, 35, 2167.
17. Santin, M.; Huang, S. J.; Iannace, S.; Ambrosio, L.; Nicolais, L.; Peluso, G. Biomaterials 1996, 17, 1459.
18. Hsieh, T. T.; Hsieh, K. H.; Simon, G. P.; Tiu, C. Polymer 1999, 40, 3153.
19. Kwok, A. Y.; Qiao, G. G.; Solomon, D. H. Polymer 2004, 45, 4017.
20. Macret, M.; Hild, G. Polymer 1982, 23, 81.
21. Kwok, A. Y.; Qiao, G. G.; Solomon, D. H. Chem Mater 2004, 16, 5650.
22. Wang, L. S.; Chow, P. Y.; Tan, D. C.-W.; Zhang, W. D. Adv Mater 2004, 16, 1790.
23. Xiang, Y. Q.; Peng, Z. Q.; Chen, D. J Eur Polym Mater 2006, 42, 2125.
24. Xing, P. X.; Ai, X.; Dong, L. S.; Feng, Z. L. Macromolecules 1998, 31, 6898.
25. Pérez, E.; Luján, M.; Salazar, J. M. Macromol Chem Phys 2000, 201, 1323.
26. Lewandowska, K. Eur Polym Mater 2005, 41, 55.
27. Zhang, X. Z.; Wu, D. Q.; Chu, C. C. Biomaterials 2004, 25, 3793.
28. Jones, D. S.; Mclaughlin, D. W. J.; McCoy, C. P.; Gorman, S. P. Biomaterials 2005, 26, 1761.
29. Sousa, R. G.; Magalhãesb, W. F.; Freitas, R. F. S. Polym Degrad Stab 1998, 61, 275.
30. Garay, M. T.; Llamas, M. C.; Iglesias, E. Polymer 1997, 38, 5091.
31. Zhang, J. T.; Huang, S. W.; Xue, Y. N.; Zhuo, R. X. Macromol Rapid Commun 2005, 26, 1346.
32. Bajpai, A. K.; Bajpai, J.; Shukla, S. J Macromol Sci Pure Appl Chem 2002, A39, 489.